Optics Communications xxx (2008) xxx–xxx

Contents lists available at ScienceDirect

Optics Communications

journal homepage: www.elsevier.com/locate/optcom

Anisotropic photonic crystals: Generalized plane wave method and dispersion symmetry properties

Irina A. Khromova [a,b,*], Leonid A. Melnikov [a]

[a] Saratov State University, Astrakhanskaya 83, Saratov 410026, Russian Federation
[b] Public University of Navarre, Campus Arrosadia, Pamplona, Navarra E31006, Spain

ARTICLE INFO

Article history:
Received 29 April 2008
Received in revised form 21 July 2008
Accepted 25 July 2008
Available online xxxx

Keywords:
Photonic crystal
Anisotropic photonic crystal
Plane wave method
Band gap

ABSTRACT

This article presents a generalized vector plane wave expansion method, applicable to isotropic and anisotropic periodic dielectric media of arbitrary geometry and dimension. The influence of anisotropic material orientation on the symmetry properties of photonic crystal dispersion surface is discussed. It is shown that the overall Brillouin zone symmetry is formed by the intersection of the photonic crystal lattice symmetry and the symmetry determined by the anisotropic material orientation. This work explains how to define the irreducible Brillouin zone of a two-dimensional anisotropic photonic crystal and demonstrates that doing it correctly allows one to avoid erroneous results, when calculating band gap diagrams of anisotropic photonic crystals. With the help of the methods presented, the possibility of controlling the band gaps of anisotropic photonic crystals by means of external electric field is shown.

1. Introduction

Photonic crystals (PCs), thanks to their unique properties and the wide range of application possibilities they offer, are nowadays among the most popular and studied objects in optics and photonics [1–5].

This work is devoted to anisotropic PCs, i.e. artificially created periodic dielectric objects with components made of anisotropic materials. PCs of this type are very interesting, as, due to their controllable dispersion, they can be used for creating tunable optical devices [6–12], in particular, devices tunable by external electric field.

This paper presents the full vector plane wave expansion method, suitable for eigenwave analysis of both isotropic and anisotropic periodic dielectric media with arbitrary geometry and dimension. It allows for tensor dielectric permittivity values and arbitrary material distributions.

The main goal of using anisotropic materials within PCs lies in the idea of external band gap control. For instance, using liquid crystals (LCs) and applying external electric field one could open or close or shift the positions of band gaps of a PC. This idea is actual for one-, two- and three-dimensional structures, as plenty of applications can be thought of for each of these cases.

One of the most popular methods used for band gap analysis is the plane wave expansion method. It is also well known that to reduce the calculation time only a part of the Brillouin zone can be taken into account. This part is a so-called irreducible Brillouin zone, which reconstructs the whole Brillouin zone when corresponding dispersion surface symmetry group operators are applied to it. For isotropic cases the symmetry of the Brillouin zone is determined only by the PC lattice symmetry, for instance, the symmetry of a two-dimensional hexagonal PC Brillouin zone is also hexagonal.

However, things get more complicated in the presence of material anisotropy. This research presents a fresh view on the anisotropic PC dispersion symmetry problem, and it will be shown below that the symmetry of an anisotropic PC dispersion surface is determined by anisotropic material orientation with respect to PC lattice vectors and/or periodicity planes.

The possibility of controlling the positions and the widths of the band gaps of anisotropic PCs by means of external electric field is also discussed in the present paper.

2. Generalized plane wave method

Several groups of methods traditionally used for PCs properties calculation can be marked out: methods, dealing with integral equations [13]; methods, representing fields in PCs as superpositions of localized functions [14]; and those, expanding field solutions into plane waves [15–19].

Localized function techniques are the most suitable methods for localized modes search, for example, it is convenient to use them when analysing defect containing structures. However, this method often appears to be rather time- and effort-consuming.

* Corresponding author. Address: Saratov State University, Astrakhanskaya 83, Saratov 410026, Russian Federation.
E-mail address: irina.khromova@unavarra.es (I.A. Khromova).

0030-4018/$ - see front matter © 2008 Elsevier B.V. All rights reserved.
doi:10.1016/j.optcom.2008.07.059

From this point of view the plane wave method is a profitable solution for calculating the dispersion properties of periodic media without defects. In particular, it is efficient and convenient for preliminary calculations when modeling complex devices based on PCs.

The presence of anisotropic materials in a PC complicates its analysis, as the dispersion equation turns from a vector one into a tensor-containing one due to the tensor magnitude of the dielectric permittivity of anisotropic media. This case does not allow using any scalar or diagonal tensor approximations, as they yield quite a rough and even erroneous solution. Moreover, these approximations do not serve for inhomogeneous distribution of anisotropic material in PC structures.

In this work, a plane wave method was generalized for anisotropic media containing PCs. This method is valid for any infinite periodic media of arbitrary dimensions, geometry, and material properties (including inhomogeneous anisotropic ones).

Consider an infinite periodic media, which in a most general case is made of a mixture of isotropic and anisotropic materials, for instance, a periodic glass walls structure, filled with LC. As it has been already mentioned, mathematically material anisotropy is expressed as a dielectric permittivity tensor, which, provided the coordinate basis coincides with anisotropy axes, looks as follows:

$$\widehat{\varepsilon}_0 = \begin{pmatrix} \varepsilon_1 & 0 & 0 \\ 0 & \varepsilon_2 & 0 \\ 0 & 0 & \varepsilon_3 \end{pmatrix}, \tag{1}$$

where ε_1, ε_2, and ε_3 characterize the material dielectric properties along each of the three directions.

Choosing any other Cartesian coordinate system results in the dielectric permittivity tensor rotation, which can be expressed as the initial tensor value $\widehat{\varepsilon}_0$ multiplied by a corresponding rotation matrix $\mathbf{T}(\bar{r})$, where $\bar{r}$ is the position vector:

$$\hat{\varepsilon}_a(\bar{r}) = \mathbf{T}(\bar{r})\hat{\varepsilon}_0(\bar{r})\mathbf{T}^{-1}(\bar{r}). \tag{2}$$

It is convenient to introduce a profile function $f(\bar{r})$ expressing the correspondence of a current coordinate position to a certain material:

$$f(\bar{r}) = \begin{cases} f_0 = 0, \text{basic media}, \\ \ldots, \\ f_i = i, \text{ material } i, \\ \ldots, \\ f_N = N, \text{material } N, \end{cases} \tag{3}$$

where N is the overall number of materials present in the structure. In a two-component glass/air case, the profile function is expressed as:

$$f(\bar{r}) = \begin{cases} f_0 = 0, \text{ air} \\ f_1 = 1, \text{ glass elements} \end{cases} \tag{4}$$

Function $f(\bar{r})$ completely describes the geometry of the periodic structure, defining the locations of isotropic and anisotropic parts, and of materials with different characteristics. Thus, using the profile function (3), one can write the expression for the inverse dielectric permittivity tensor distribution $\hat{\eta}(\bar{r}) = \hat{\varepsilon}^{-1}(\bar{r})$ as follows:

$$\hat{\eta}(\bar{r}) = \hat{\eta}_0(\bar{r})\frac{\prod_{j=1}^{N}(f(\bar{r})-j)}{\prod_{j=1}^{N}(f_0-j)} + \sum_{i=1}^{N=1}\hat{\eta}_i(\bar{r})\frac{\prod_{j=0}^{i-1}(f(\bar{r})-j)\prod_{j=i+1}^{N}(f(\bar{r})-j)}{\prod_{j=0}^{i-1}(f_i-j)\prod_{j=i+1}^{N}(f_i-j)} + \hat{\eta}_N(\bar{r})\frac{\prod_{j=0}^{N-1}(f(\bar{r})-j)}{\prod_{j=0}^{N=1}(f_N-j)} \tag{5}$$

In every coordinate point all but one item of this sum turn to zero. The nonzero item corresponds to the value of the inverse dielectric permittivity of the material, which is located in the point concerned. In a two-component PC case expression (5) looks as follows:

$$\hat{\eta}(\bar{r}) = \hat{\eta}_{\text{glass}} f(\bar{r}) + \hat{\eta}_{\text{a}}(\bar{r})(1 - f(\bar{r})), \tag{6}$$

where $\hat{\eta}_{\text{a}}(\bar{r}) = \hat{\varepsilon}_{\text{a}}^{-1}(\bar{r})$ is the inverse dielectric permittivity tensor of the anisotropic material (2), $\hat{\eta}_{\text{glass}} = \begin{pmatrix} \frac{1}{\varepsilon_{\text{glass}}} & 0 & 0 \\ 0 & \frac{1}{\varepsilon_{\text{glass}}} & 0 \\ 0 & 0 & \frac{1}{\varepsilon_{\text{glass}}} \end{pmatrix}$ is the inverse dielectric permittivity tensor of the isotropic material (glass) characterized by the scalar value of the dielectric permittivity $\varepsilon_{\text{glass}}$. Knowing that the inverse dielectric permittivity tensor can be easily obtained for every coordinate point from Eqs. (5) and (6), and denoting the free-space wavelength as λ, one can describe the behaviour of the magnetic field by a Helmholtz equation

$$\nabla \times (\hat{\eta}(\bar{r})\nabla \times \bar{H}(\bar{r})) = \left(\frac{2\pi}{\lambda}\right)^2 \bar{H}(\bar{r}) \tag{7}$$

In the plane wave method the solution of Eq. (7) is represented in the form of a plane wave superposition:

$$\bar{H}(\bar{r}) = \exp(\mathrm{i}\bar{k}\bar{r}) \sum_{\bar{G}} \bar{H}_{\bar{G}} \exp(\mathrm{i}\bar{G}\bar{r}), \tag{8}$$

where $\bar{G}$ is the PC reciprocal lattice vector, $\bar{k}$ is the Bloch vector, and $\bar{H}_{\bar{G}}$ is the magnetic field plane wave expansion amplitude.

The third Maxwell's equation $\mathrm{div}\bar{H}(\bar{r}) = 0$ states that vector $\bar{H}_{\bar{G}}$ is orthogonal to vector $\bar{e}_3 = \frac{\bar{k}+\bar{G}}{|\bar{k}+\bar{G}|}$. Therefore, a specially chosen coordinate system can allow one to reduce the number of nonzero components of vector $\bar{H}_{\bar{G}}$ [15–18] and, consequently, the number of equations to be solved. Introducing two orthogonal vectors $\bar{e}_1$ and $\bar{e}_2$, each of them being orthogonal to vector $\bar{e}_3$ and depending on the reciprocal lattice vector $\bar{G}$ so that $\bar{H}_{\bar{G}} = \bar{H}_{\bar{G}}^{(1)}\bar{e}_1 + \bar{H}_{\bar{G}}^{(2)}\bar{e}_2$, one can rewrite Eq. (7) in the basis of $(\bar{e}_1, \bar{e}_2, \bar{e}_3)$ as a matrix equation:

$$\sum_{\bar{G}'} \left|\vec{k}+\vec{G}\right| \cdot \left|\vec{k}+\vec{G}'\right| \mathbf{M} \begin{pmatrix} H_{\bar{G}'}^{(1)} \\ H_{\bar{G}'}^{(2)} \end{pmatrix} = -\left(\frac{2\pi}{\lambda}\right)^2 \begin{pmatrix} H_{\bar{G}}^{(1)} \\ H_{\bar{G}}^{(2)} \end{pmatrix}, \tag{9}$$

where $\mathbf{M}$ is a matrix containing the Fourier components of the inverse dielectric permittivity tensor $\hat{\eta}_{\bar{G}}$. In a most general case it looks as follows:

$$\mathbf{M} = \begin{pmatrix} \bar{e}_1^{\bar{G}'} \cdot \left[\bar{e}_2^{\bar{G}} \times \left(\hat{\eta}_{\bar{G}-\bar{G}'} \cdot \bar{e}_2^{\bar{G}'}\right)\right] & -\bar{e}_1^{\bar{G}} \cdot \left[\bar{e}_2^{\bar{G}} \times \left(\hat{\eta}_{\bar{G}-\bar{G}'} \cdot \bar{e}_1^{\bar{G}'}\right)\right] \\ \bar{e}_2^{\bar{G}'} \cdot \left[\bar{e}_2^{\bar{G}} \times \left(\hat{\eta}_{\bar{G}-\bar{G}'} \cdot \bar{e}_2^{\bar{G}'}\right)\right] & -\bar{e}_2^{\bar{G}'} \cdot \left[\bar{e}_2^{\bar{G}} \times \left(\hat{\eta}_{\bar{G}-\bar{G}'} \cdot \bar{e}_1^{\bar{G}'}\right)\right] \end{pmatrix} \tag{10}$$

When the anisotropic material infilling is homogeneous, i.e. when the anisotropic material molecules' orientation does not depend on coordinates $\hat{\eta}_{\text{a}}(\bar{r}) = \hat{\eta}_{\text{a}}$, all the Fourier transformation process goes to the profile function $f(\bar{r})$ (3,4). For instance, in the two-component case (4) the general expression for the Fourier components of the inverse dielectric permittivity tensor is as follows:

$$\hat{\eta}_{\bar{G}} = f_{\bar{G}}(\hat{\eta}_{\text{glass}} - \hat{\eta}_{\text{a}}) + \delta(\bar{G})\hat{\eta}_{\text{a}} \tag{11}$$

where $f_{\bar{G}}$ is a Fourier component of the profile function $f(\bar{r})$. Substituting the latter relation into Eq. (10), one can calculate the matrix $\mathbf{M}$ with a significant saving of time.

Solving the eigenvalue problem (9) yields a set of eigennumbers (inverse wavelengths) for every certain Bloch vector $\bar{k}$, the magnitude of which is set within the first Brillouin zone of the considered PC. A photonic band gap appears, when for all of the Bloch vectors within the Brillouin zone there are no real eigenvalues, which means that any propagation direction is forbidden for a range of

Please cite this article in press as: I.A. Khromova, L.A. Melnikov, Opt. Commun. (2008), doi:10.1016/j.optcom.2008.07.059

frequencies (in a two-dimensional case it means that any propagation direction is forbidden for a certain propagation constant for a range of frequencies).

Using the method described above, one can rapidly calculate the dispersion diagram of a PC with arbitrary geometry, dimension and dielectric properties. Further on, a more precise and time-consuming method can be applied to obtain the desired dispersion characteristics in a more accurate way [5,18].

The results given below were obtained by means of the described generalized plane wave method, realized as a FORTRAN language algorithm.

3. Symmetry of anisotropic PC Brillouin zone

In order to determine the positions and widths of band gaps, it is necessary to know the values of the boundary frequencies or wavelengths, between which there are no real eigenproblem (9) solutions. In the isotropic case, these frequency values lie on the boundary of the irreducible Brillouin zone, determined by the PC lattice symmetry. This Section shows how the symmetry of the dispersion surface is influenced by the anisotropy of PC component materials. The stated problem will be considered for the case of two-dimensional PCs, as they are widely used, e.g. in PC fibers [4,5,8,9], and are very important for modern optics and photonics.

The dispersion surface of a two-dimensional PC is a three-dimensional surface, as it is the dependence of the wavelength (or frequency or freespace wavevector magnitude) on the two-dimensional Bloch vector. It is defined for every fixed value of the third non-Bloch component of the wavevector. The two-dimensional PC dispersion surface is a complicated surface with gaps along the frequency (wavelength) axis. As it is known, the dispersion surface extreme points are located in the symmetry points and along the symmetry axes of the Brillouin zone of a certain PC.

Fig. 1 shows different dispersion surface layers (solutions of eigenproblem (9), yielding the dependence of $K = 2\pi/\lambda$, where λ is the wavelength, on the Bloch vector components (k_x, k_y)) calculated by the method described above for the isotropic kagome-type PC [21] with the period of $p = 2\ \mu m$, glass wall thickness of $\Delta = 300$ nm and glass refractive index $n = 1.52$. The air gaps between the glass walls are filled with an isotropic material with refractive index $n' = 1.4$. For convenience further on in this paper, we will consider only this geometry. In Fig. 1, the scale varies from one contour plot to another for the purpose of comprehension convenience, while the number of equal value levels is the same throughout all the paper and equals to 15. The maxima and minima on these grey-scale contour graphs are denoted by dark grey colour and white colour correspondingly. The triangle $\Gamma MK\left\{(0,0),\left(0,2\pi/p\sqrt{3}\right),\left(2\pi/p,2\pi/p\sqrt{3}\right)\right\}$ is the irreducible Brillouin zone boundary. It serves as an elementary part of the Brillouin zone and can reconstruct the whole zone completely after being processed by the D_6 symmetry operations (which are the hexagonal lattice symmetry group operations). The boundary of the irreducible Brillouin zone contains all the extreme points of the dispersion surface, and it is therefore possible to find the positions of band gaps only by solving the eigenproblem (9) for the Bloch vector components belonging to the irreducible Brillouin zone boundary (instead of considering the whole Brillouin zone).

The simplest way to make the considered PC anisotropic is to fill the air gaps between the glass walls with an LC. In this paper, we assume that it is a nematic LC with refractive indices equal to $n_{||} = 1.7$, $n_{\perp} = 1.4$.

In the presence of anisotropy, the scalar dielectric permittivity description is no longer valid. It can be easily explained, if one considers a two-dimensional PC (Fig. 2) as a three-dimensional object (Fig. 3).

Fig. 3 shows a schematic "element" of a two-dimensional PC: a hollow glass tube, which can be filled with anisotropic material, and the equivalent three-dimensional Brillouin zone and its irreducible part. The three-dimensional Brillouin zone has arbitrary height due to the PC's zero-period along the z-axis (the axis perpendicular to the PC periodicity plane) [17]. For simplicity in this paper only uni-axial anisotropy like that of the LC will be considered, although similar conclusions can be drawn for other types of anisotropic materials. It has already been mentioned that the coordinate system was chosen to have the z-axis perpendicular to the (x,y) PC periodicity plane, the x-axis parallel to one of the

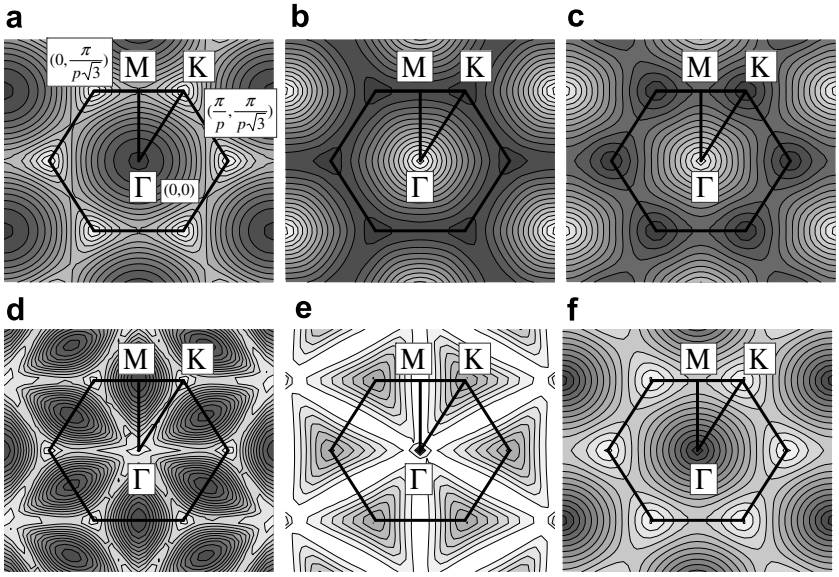

Fig. 1. Contour plots of different roots of the dispersion equation (9) for the isotropic kagome-lattice PC. The symmetry of the Brillouin zone coincides with the PC lattice symmetry. The black solid line denotes the Brillouin zone and its irreducible part (the ΓMK triangle). The wavenumber minima $K_{min} = 2\pi/\lambda_{max}$ (denoted by dark grey) and maxima $K_{max} = 2\pi/\lambda_{min}$ (denoted by white) correspond to the following values: (a) $K_{min} = 13.86$ rad/μm, $K_{max} = 13.91$ rad/μm; (b) $K_{min} = 13.91$ rad/μm, $K_{max} = 14.02$ rad/μm; (c) $K_{min} = 13.91$ rad/μm, $K_{max} = 14.03$ rad/μm; (d) $K_{min} = 14.01555$ rad/μm, $K_{max} = 14.0210$ rad/μm; (e) $K_{min} = 14.015$ rad/μm, $K_{max} = 14.027$ rad/μm; (f) $K_{min} = 14.02$ rad/μm, $K_{max} = 14.18$ rad/μm.

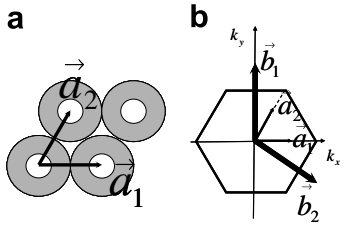

Fig. 2. (a) A schematic view of a two-dimensional PC hexagonal lattice, $\bar{a}_1, \bar{a}_2$ are the translation vectors, (b) Reciprocal lattice vectors $\bar{b}_1, \bar{b}_2$ and the Brillouin zone.

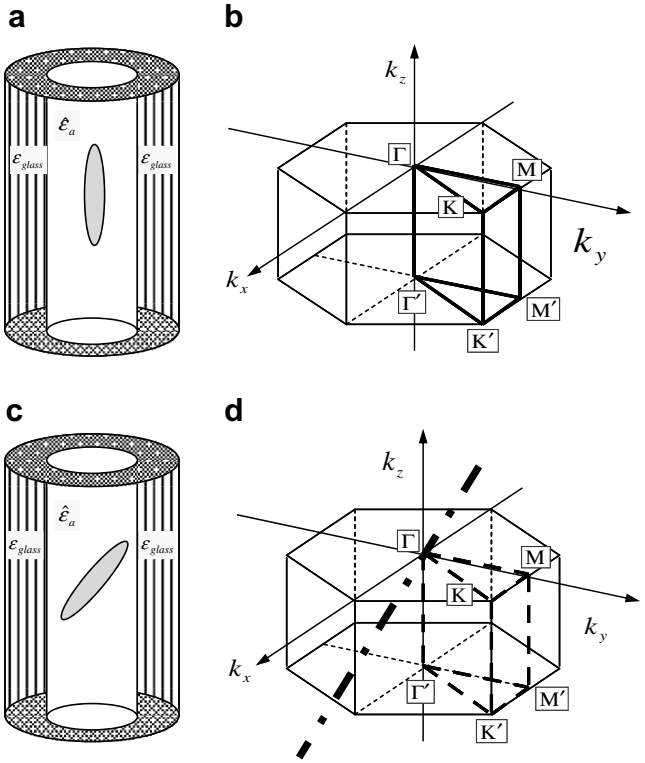

Fig. 3. (a,c) Sketches of a two-dimensional anisotropic PC element: a glass wall capillary. The ellipses denote the LC molecules oriented along the PC-axis (z-axis) and oriented arbitrary correspondingly. (b,d) Equivalent tree-dimensional Brillouin zone for the anisotropic director perpendicular orientation and arbitrary orientation correspondingly. The solid line denotes the irreducible Brillouin zone, the dashed line shows the same "isotropic" irreducible Brillouin zone, which is not correct for arbitrary anisotropic molecules orientation, the dot-dashed line shows the LC director orientation, which gives rise to a Brillouin zone special direction appearance.

PC translation vectors (in our case $\bar{a}_1$, see Fig. 2), and the y-axis lying in the PC periodicity plane.

The symmetry of the Brillouin zone is determined by both the PC lattice symmetry and the symmetry of the dielectric permittivity tensor with respect to the PC periodicity plane and lattice vectors.

When the anisotropic material is oriented along the z-axis, i.e. when any vector $\bar{d}$ belonging to the anisotropic material director orientation line has a zero projection on the PC periodicity plane, $\bar{d}_{(x,y)} = \bar{0}$, the situation is identical to the isotropic case: the dielectric permittivity ellipsoid yields the $O(2)$ symmetry group, which, intersected with any PC lattice symmetry group, simply gives the unchanged PC lattice symmetry group. Thus, the Brillouin zone in this case has the same symmetry as that of the PC lattice, that is, the D_6 symmetry for the considered hexagonal lattice case.

When anisotropic material molecules reorient themselves, the symmetry of the dielectric permittivity tensor changes, which leads to the overall Brillouin zone symmetry change (Fig. 3b).

Consider the rotation of a uni-axial anisotropic material dielectric permittivity tensor. This process involves a nonzero periodicity plane projection appearance $\bar{d}_{(x,y)} \neq \bar{0}$. When $\bar{d}_{(x,y)}$ coincides with any PC lattice translation vector direction, the symmetry group with respect to the chosen coordinate system turns into a dihedral one $D_1 \cap D_6 = D_1$. Consider, for instance, the director rotation around the x-axis. It produces a nonzero $\bar{d}_{(x,y)} || (-\bar{a}_1 + 2\bar{a}_2)$, $m, n \in N$. In a most general case of out-of-plane propagation (with nonzero k_z) due to the overall "three-dimensionality" of the system considered, the x-axis symmetry will no longer be conserved. The dihedral y-axis symmetry means that two waves with equal y- and z-wavevector components and opposite and absolutely equal x-components have the same frequency, i.e. they face equal propagation conditions (see Fig. 4a). However, two waves with equal x- and z-wavevector components, but opposite and absolutely equal y-wavevector components will face distinct dielectric permittivity values (Fig. 4b).

3.1. Out-of-plane LC orientation with director projection along a PC lattice vector

Fig. 5 shows one and the same dispersion surface layer (solution of eigenproblem (9)) for the kagome lattice with air gaps homogeneously filled with LC (refractive indices $n_{||} = 1.7$, $n_{\perp} = 1.4$) *at different angles of LC director orientation with respect to the z-axis in the (x,z)-plane (containing the z-axis and the $\bar{a}_1$ lattice translation vector).*

The symmetry order rises up to $D_2 = D_2 \cap C_6$ when the LC director is oriented within the PC periodicity plane, so that $\bar{d}_{(x,y)} || (m\bar{a}_1 + n\bar{a}_2)$, $m, n \in \mathbf{N}$ and $d_z = 0$, due to the appearance of a second symmetry axis, perpendicular to the LC director orientation. This effect is shown in Fig. 5e, where the irreducible Brillouin zone is $\Gamma K M_1 M_2$ and in Fig. 6, where several dispersion surface layers are shown for the same angle of the in-plane LC director orientation.

3.2. In-plane LC orientation

Another particular case is when the LC director is oriented arbitrarily within the PC periodicity plane, i.e. in the (x,y) plane. An arbitrary in-plane LC director orientation, not parallel to any of the PC lattice translation vectors, i.e. such as $(\forall(n,m) \in \mathbf{N}) \neg (\bar{d}_{(x,y)} || (m\bar{a}_1 + n\bar{a}_2))$ and $d_z = 0$, destroys the D_i-type symmetry and converts it into a circular one, which in this particular case is $C_2 \cap D_6 = C_2$.

Fig. 7 shows contour plots of one particular layer of the dispersion surface calculated for different angles of LC director in-plane orientation. The reasons of the symmetry type change are the same as in the previous case. The particular thing about the arbitrary in-plane orientation is that due to circular symmetry it is no longer possible to define a unique irreducible Brillouin zone. For the same reason there are no special contours and points containing all the extreme points of the dispersion surface. Fig. 8 shows the contour plots of a dispersion surface layer, different from the one shown in Fig. 7, at the same LC director orientation angles. It can be noticed that the locations of the extreme points in the plots of Fig. 8 do not coincide with those shown in Fig. 7.

In this case, in order to find the boundaries of the band gaps, one should carry out calculations over one half of the Brillouin zone. Figs. 7a, d, f and 8a, d, f show the in-plane LC director orientation, parallel to a PC lattice vector, these cases were already discussed in the previous Section and correspond to the second order dihedral symmetry $D_2 \cap D_6 = D_2$.

Please cite this article in press as: I.A. Khromova, L.A. Melnikov, Opt. Commun. (2008), doi:10.1016/j.optcom.2008.07.059

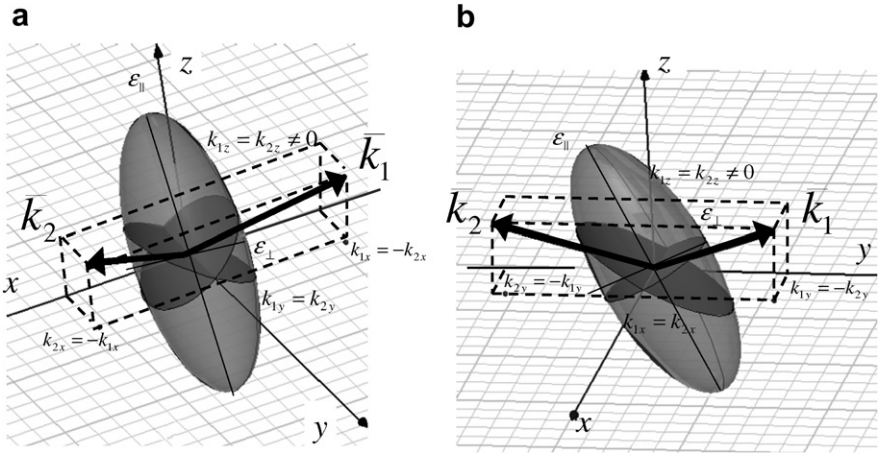

Fig. 4. Ellipsoid of the dielectric permittivity tensor inclined at a 25° angle with respect to the z-axis in the (y,z) plane. (a) waves with equal $k_{1z} = k_{2z}, k_{1y} = k_{2y}$ wavevector components and equal absolute values of the third wavevector component $k_{1x} = -k_{2x}$ face the same propagation conditions; (b) for the waves with $k_{1z} = k_{2z}, k_{1x} = k_{2x}$ and $k_{1y} = -k_{2y}$ the propagation conditions become distinct. The mirror symmetry is destroyed.

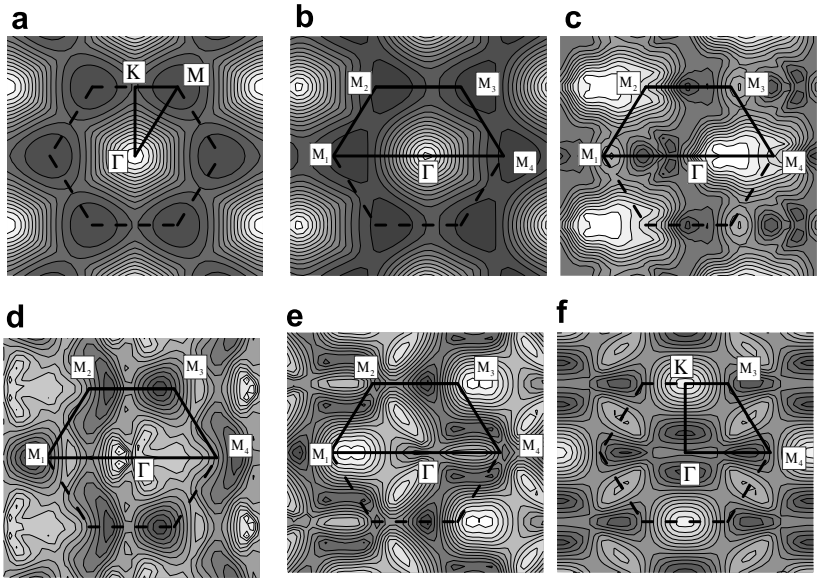

Fig. 5. Dispersion surface layer contour plots. LC director is orientated within the (x,i) plane at different angels with respect to the z-axis (a) $\alpha = 0°$ (identical to the isotropic case), (b) $\alpha = 10°$ (D_6) symmetry), (c) $\alpha = 30°$ (D_1 symmetry), (d) $\alpha = 60°$ (D_1 symmetry), (e) $\alpha = 70°$ (D_1 symmetry), (f) $\alpha = 90°$, along the $\bar{a}_1$-vector (D_2 symmetry). The dashed line denotes the Brillouin zone, the solid line marks its irreducible part. The Brillouin zone symmetry is disturbed by the anisotropic material.

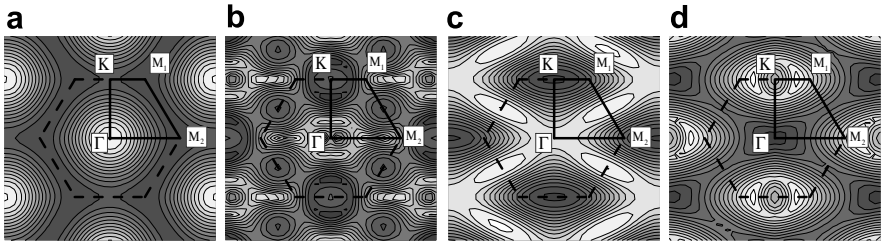

Fig. 6. Different layers of the dispersion surface in the case of LC in-plane orientation (along the $\bar{a}_1$ lattice translation vector). The dashed line shows the Brillouin zone boundary, the solid line marks its irreducible part. The symmetry order rises up to D_2.

3.3. Out-of-plane arbitrary LC orientation

There is one more case left to consider: an arbitrary LC director orientation, when vector $\bar{d}$ has a nonzero z-component and its projection on the PC periodicity plane is not parallel to any of the PC lattice translation vectors, i.e. $(\forall(n,m) \in \mathbf{N})\neg(\bar{d}_{(x,y)} || (m\bar{a}_1 + n\bar{a}_2))$ and $d_z \neq 0$. In this case, it is impossible to define an irreducible Brillouin zone part due to absence of any symmetry except the trivial one $C_1 \cap D_6 = C_1$ (Fig. 9).

All conclusions presented above can be drawn for any type of PC lattice (triangular, quadratic and hexagonal) with the only difference that when intersecting the PC lattice symmetry group with

Please cite this article in press as: I.A. Khromova, L.A. Melnikov, Opt. Commun. (2008), doi:10.1016/j.optcom.2008.07.059

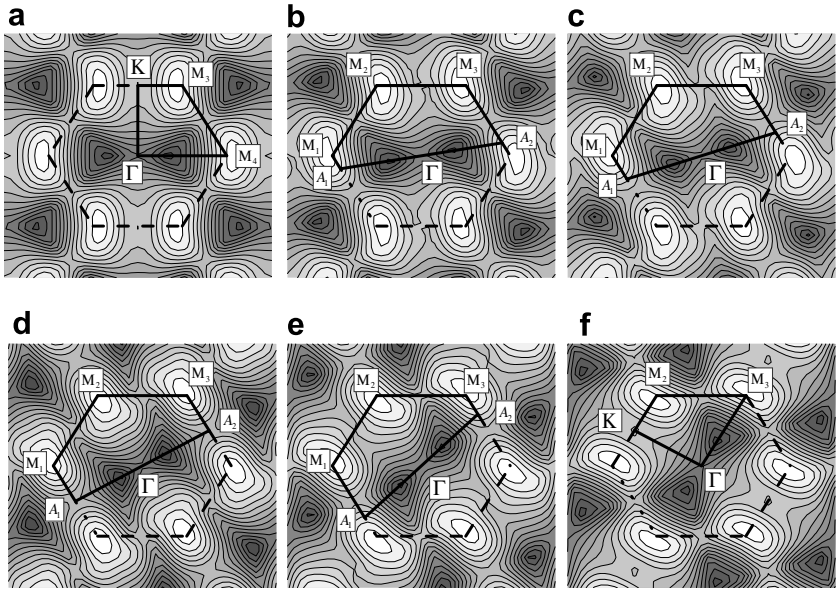

Fig. 7. Dispersion surface layer contour plots. The LC director is oriented within the PC periodicity plane at the following angles to the $\bar{a}_1$ translation vector: (a) $\alpha = 0°$ (parallel to $\bar{a}_1$), (b) $\alpha = 10°$, (c) $\alpha = 20°$, (d) $\alpha = 30°$ (parallel to $\bar{a}_1 + \bar{a}_2$), (e) $\alpha = 45°$, (f) $\alpha = 60°$ (parallel to $\bar{a}_2$). The dashed line denotes the Brillouin zone boundary and the solid line marks its irreducible part. The dihedral symmetry turns into a circular one.

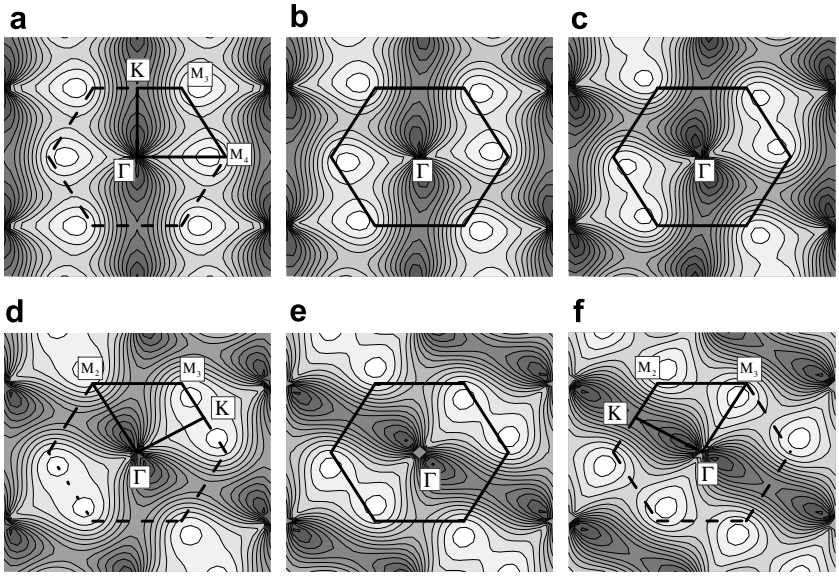

Fig. 8. Dispersion surface layer different from the one shown in Fig. 7. LC director is oriented within the PC periodicity plane at the following angles to the $\bar{a}_1$ translation vector: (a) $\alpha = 0°$ (parallel to $\bar{a}_1$), (b) $\alpha = 10°$, (c) $\alpha = 20°$, (d) $\alpha = 30°$ (parallel to $\bar{a}_1 + \bar{a}_2$), (e) $\alpha = 45°$, (f) $\alpha = 60°$ (parallel to $\bar{a}_2$). The dashed line shows the Brillouin zone boundary, and the solid line marks its irreducible part. The positions of the dispersion surface layer extreme points differ from those shown in Fig. 7.

the symmetry group determined by the LC orientation, one would have to substitute a corresponding lattice symmetry group for the D_6 symmetry group, which describes the discussed hexagonal PC lattice symmetry case.

3.4. Summary on irreducible Brillouin zones

Summing up all the cases considered and denoting an arbitrary two-dimensional lattice symmetry group as G_{PC}, four main cases of uni-axial anisotropic material orientation can be outlined:

1. When an arbitrary vector $\bar{d}$ belonging to the LC director orientation line is parallel to one of the PC lattice translation vectors, i.e. $\bar{d}_{(x,y)} || (m\bar{a}_1 + n\bar{a}_2),\ m, n \in \mathbf{N}$, and lies within the PC periodicity plane, i.e. $d_z = 0$, the Brullouin zone symmetry is determined as $D_2 \cap G_{PC}$.
2. When $\bar{d}$ lies within the PC periodicity plane and is not parallel to any of the PC lattice translation vectors, i.e. $(\forall(n, m) \in \mathbf{N}) \neg (\bar{d}_{(x,y)} || (m\bar{a}_1 + n\bar{a}_2))$ and $d_z = 0$, the Brullouin zone symmetry is determined as $C_2 \cap G_{PC}$.
3. When $\bar{d}$ does not belong to the PC periodicity plane, but its projection on the PC periodicity plane is parallel to one of the PC lattice translation vectors, i.e. $\bar{d}_{(x,y)} || (m\bar{a}_1 + n\bar{a}_2),\ m, n \in \mathbf{N}$ and $d_z \neq 0$, the Brullouin zone symmetry is determined as $D_1 \cap G_{PC}$.
4. When $\bar{d}$ does not belong to the PC periodicity plane and its projection on the PC periodicity plane is not parallel to any of the PC lattice translation vectors, i.e. $(\forall(n, m) \in \mathbf{N}) \neg (\bar{d}_{(x,y)} || (m\bar{a}_1 +$

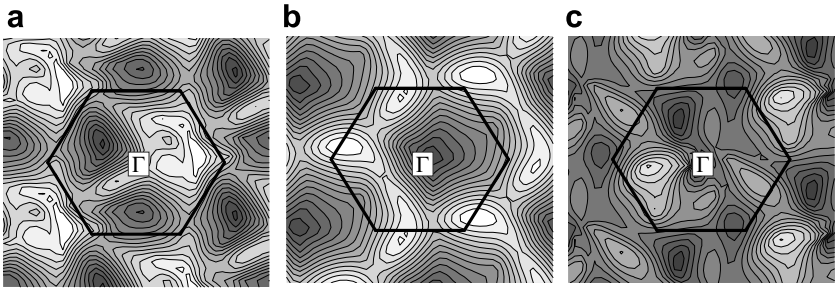

Fig. 9. Different dispersion surface layers in the case of arbitrary LC director orientation, when no irreducible Brillouin zone can be defined. The LC director orientation is not parallel to any of the PC lattice translation vectors: (a) $\alpha_1 = 60°$ with respect to the z-axis and $\alpha_2 = 20°$ with respect to vector $\bar{a}_1$, (b) $\alpha_1 = 30°$ with respect to the z-axis and $\alpha_2 = 35°$ with respect to vector $\bar{a}_1$, (c) $\alpha_1 = 45°$ with respect to the z-axis and $\alpha_2 = 20°$ with respect to vector $\bar{a}_1$. The Brillouin zone is marked by the solid line. In this most general case only the trivial symmetry $C_1 \cap D_6 = C_1$ is left.

$n\bar{a}_2$)) and $d_z \neq 0$, the Brullouin zone symmetry is determined as $C_1 \cap G_{PC} = C_1$.

In case of dihedral symmetry D_i the boundary of the corresponding irreducible Brillouin zone contains all the dispersion surface extreme points, therefore, for band gap analysis one can consider only the Bloch vector components, corresponding to the irreducible Brilloin zone boundary.

In case of circular symmetry C_i due to non-uniqueness of the irreducible Brillouine zone all points of the ith part of the Brillouin zone should be taken into account for band gap analysis, as the positions of dispersion surface extreme points can hardly be predicted.

4. Importance of correct irreducile Brillouin zone choice

Many works devoted to the anisotropic PC problem ignore the principal difference between isotropic and anisotropic PCs and follow the "isotropic symmetry ideas" or consider only the in-plane propagation [6,7,20] when analysing for both of the cases. This Section shows why it is important to perform the band gap analysis using the full tensor approach and the correctly chosen irreducible Brillouin zone.

Whenever the anisotropic material main axes do not coincide with the working coordinate system basis, the diagonal tensor approach gives erroneous result, simply because in this case the dielectric permittivity tensor is no longer diagonal.

Using the "isotropic" irreducible Brillouin zone (determined only by the PC lattice symmetry) for anisotropic PCs is incorrect and provokes errors in dispersion calculations. Fig. 10 compares the band gap diagrams of the considered anisotropic PC, calculated over the correct irreducible Brillouin zone, defined according to the approach presented above (Fig. 10a), and those, calculated over the conventional "isotropic" irreducible Brillouin zone (Fig. 10b). To demonstrate the accuracy of the approach, both of the diagrams are compared with the band gap diagram, calculated over all the points of the Brillouin zone (denoted by grey colour in Fig. 10a,b).

The band gap diagrams coincide in Fig. 10a and differ in Fig. 10b. For instance, the gaps between the black areas in Fig. 10b do not always correspond to real band gaps, which are the gaps between the grey areas in Fig. 10b. This fact proves that the conventional "isotropic" approach to anisotropic photonic crystals gives erroneous results, while choosing the irreducible Brillouin zone correctly, as it is recommended in the paper, helps to obtain accurate band gap diagrams, equivalent to those calculated over the whole Brillouin zone.

5. Anisotropic PC band gap control

This Section demonstrates the possibility of changing the positions and widths of anisotropic PC band gaps by means of anisotropic material reorientation [22–24]. For calculations, the same kagome-lattice PC, described in Section 3, was used.

Fig. 11 shows how a band gap diagram of an anisotropic PC can change with the anisotropic material reorientation. The reorientation shown in the figure corresponds to the type considered in Section 3.1. It is an out-of-plane LC director rotation, with the projection of the latter on the PC periodicity plane being parallel

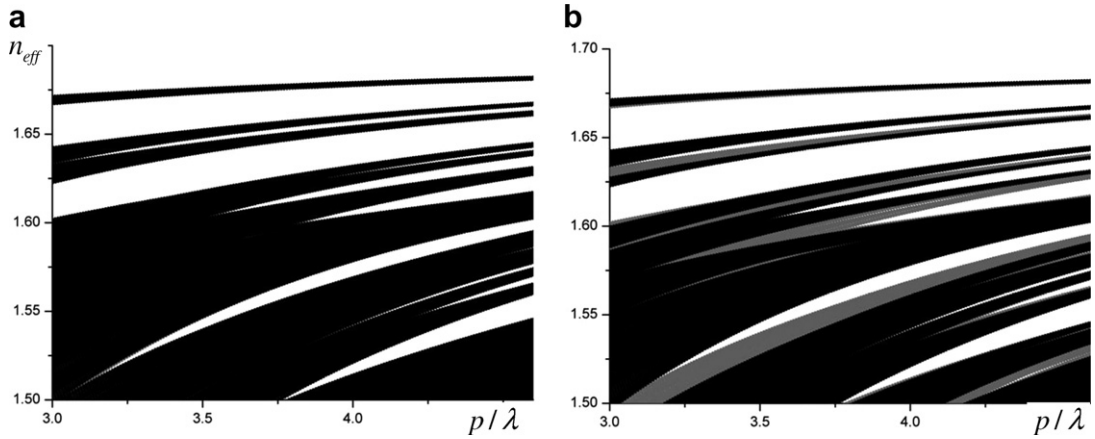

Fig. 10. Comparing the band gap diagrams, calculated over the correct irreducible Brillouin zone (black, a) and over the conventional "isotropic" (black, b) one with the true band gap diagram, calculated over the whole Brillouin zone (grey, a,b). White areas correspond to band gaps. The LC director is oriented out-of-plane (in the (x,z)-plane) at an angle of $\alpha = 85°$ to the z-axis. n_{eff} is the effective refractive index, p/λ is the structure period/wavelength relation. The presented approach yields no errors, while the conventional one does.

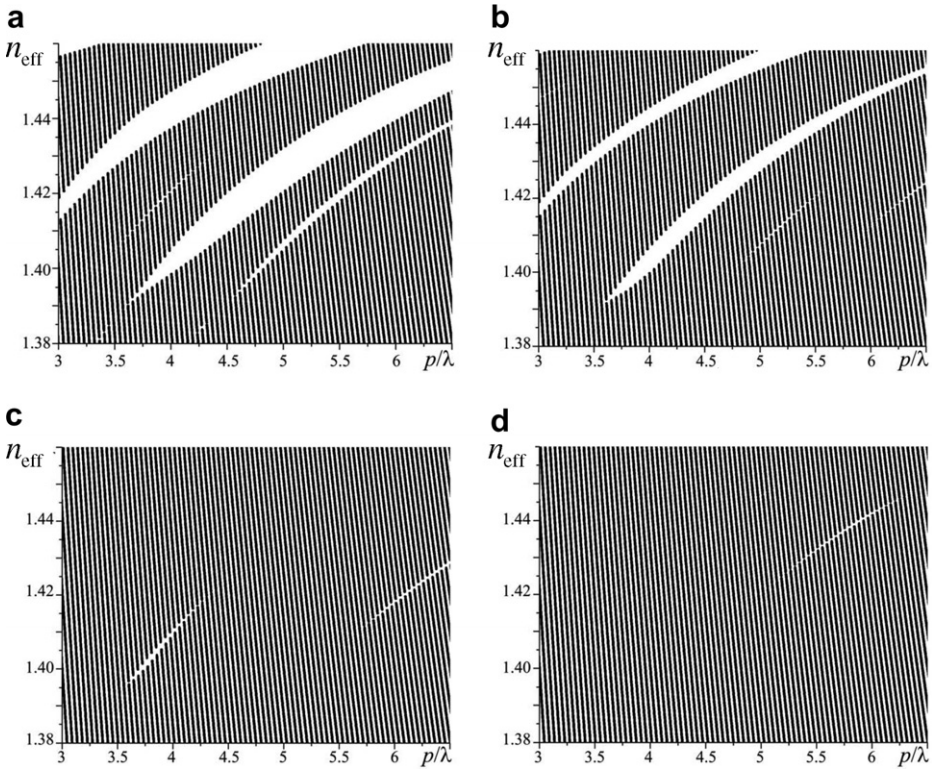

Fig. 11. Band gap diagrams of LC infilled kagome-lattice PC with LC director oriented at different angles to the longitudinal PC-axis (case described in Section 3.1): (a) $\alpha = 0°$, (b) $\alpha = 5°$, (c) $\alpha = 10°$, (d) $\alpha = 15°$. n_{eff} is the effective refractive index, p/λ is the structure period/wavelength relation. White areas correspond to photonic band gaps. LC reorientation leads to a considerable change in the positions and widths of the band gaps.

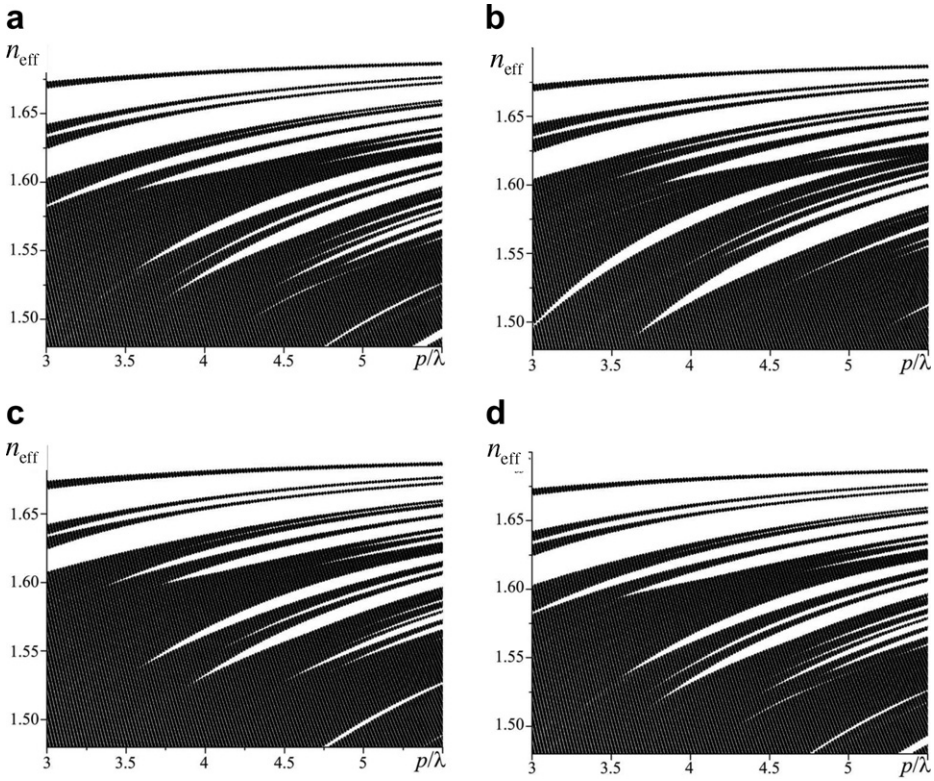

Fig. 12. Band gap diagrams of the LC infilled kagome-lattice PC with LC director oriented in-plane at different angles to one of the PC lattice vectors (case described in Section 3.2): (a) $\alpha = 0°$, (b) $\alpha = 10°$, (c) $\alpha = 30°$, (d) $\alpha = 60°$. n_{eff} is the effective refractive index, p/λ is the structure period/wavelength relation. White areas correspond to photonic band gaps. LC reorientation leads to a considerable change in the positions and widths of the band gaps.

Please cite this article in press as: I.A. Khromova, L.A. Melnikov, Opt. Commun. (2008), doi:10.1016/j.optcom.2008.07.059

to one of the PC lattice vectors. Fig. 12 presents the band gap diagrams of the same anisotropic PC at LC director in-plane rotation. This case corresponds to the one considered in Section 3.2. It can be seen from these figures that reorienting the anisotropic material director (by means of external electric field) can modify the band gap diagram of an anisotropic PC, i.e. it can open/close or shift the band gaps or change their widths.

6. Conclusion

In this work, a generalized vector plane wave method applicable to isotropic and anisotropic PC of arbitrary geometry and dimension was presented. It allows one to perform band gap analyses of any sort of infinite periodic structures and, with the help of other methods (supercell method, finite elements method, etc.), to calculate the properties of complex PC based objects, such as PC waveguides or defect containing PC structures [16].

The dramatic influence of material anisotropy on the Brillouin zone symmetry was demonstrated. It was shown that the overall dispersion surface symmetry if formed by both the PC lattice symmetry and the symmetry, determined by the anisotropic material orientation with respect to the PC lattice translation vectors and/or periodicity planes.

To perform the band gap analysis of an anisotropic PC correctly one can either take all the points of the Brillouin zone into account or consider only the points of the irreducible Brillouin zone. The first approach, although it certainly yields a correct band gap diagram, is a rather time-demanding one. The success of second way, which helps to save time and computational costs, depends on the accuracy of the irreducible Brillouin zone choice. This paper showed how to define the irreducible Brillouin zone correctly for a two-dimensional PC infilled with a uni-axial anisotropic material.

Four main cases of homogeneous anisotropic material director orientation were outlined: the in-plane director orientation with its projection on the PC periodicity plane being parallel to one of the PC lattice vectors; the out-of-plane director orientation with its projection on the PC periodicity plane being parallel to one of the PC lattice vectors; the arbitrary in-plane orientation; and the arbitrary out-of-plane orientation. In each of these cases a certain Brillouin zone symmetry appears: second-order dihedral D_2; first-order dihedral D_1; second-order circular C_2; and trivial C_1 correspondingly (for the hexagonal PC lattice).

In case of the circular symmetry of the Brillouin zone (including the trivial one), it is not possible to define the irreducible Brillouin zone unambiguously and all the points of the corresponding *i*th part of the whole Brillouin zone should be taken into account for band gap analysis, as any of them may contain a dispersion surface extreme point. It means that in a most general case, which is characterized by the trivial Brillouin zone symmetry, all possible Bloch vector components should be considered in order to perform the calculations correctly.

Following the presented approach one can avoid errors produced by dispersion extreme point skipping and to reduce the calculation time, as there are cases, when certain Brillouin zone symmetry exists and, thus, there is no necessity to perform calculations over all possible Bloch vector components.

It is important to be able to analyse such complicated anisotropic structures, because, as it was demonstrated in this paper, they offer the possibility to control the photonic band gaps externally, without changing the geometry of the PC structure or the dielectric properties of the PC component materials.

References

[1] J.D. Joannopoulos, P.R. Villeneuve, S. Fan, Nature (London) 386 (1997) 143.
[2] K.M. Ho, C.T. Chan, C.M. Soukoulis, Physical Review Letters 65 (1990) 3152.
[3] P.J. Russell, T.A. Birks, F.D. Lloyd-Lucas, Photonic Bloch waves and photonic band gaps, in: Confined Electrons and Photons: New Physics and Applications, 1995, p. 585.
[4] J.C. Knight, J. Broeng, T.A. Birks, P.S.J. Russell, Science 282 (5393) (1998) 1476.
[5] J. Arriaga, J.C. Knight, P.St.J. Russell, Physica E17 (2003) 440.
[6] Zh.-Yu. Li, L.-L. Lin, B.-Yu. Gu, Gu.-Zh. Yang, Physica B279 (2000) 159.
[7] Young-Chung Hsue, Ben-Yuan Gu, The Extended Plane Wave Expansion Method in Three Dimensional Anisotropic Photonic Crystal, 2004. arxiv:/arXiv:physics/0405026v1.
[8] T.T. Larsen, Optics Express 11 (20) (2003) 2589.
[9] T.T. Alkeskjold, Optics Express 12 (24) (2004) 5857.
[10] F. Du, Y.-Q. Lu, S.-T. Wu, Applied Physics Letters 85 (12) (2004) 2181.
[11] R. Kotynski et al., Modeling of polarization behaviour of LC filled PC fibers, in: Proceedings Symposium IEEE/LEOS Benelux Chapter, 2004, p. 315.
[12] L. Scolari, Optics Express 13 (19) (2005) 7483.
[13] F. Seydou et al., Optics Express 14 (23) (2006) 11362.
[14] K. Busch et al., Journal of Physics: Condensed Matter 15 (2003) 1233.
[15] S.G. Johnson, J.D. Joannopoulos, Optics Express 8 (3) (2001) 173.
[16] Sh. Guo, S. Albin, Optics Express 11 (2) (2003) 167.
[17] M. Løkke et al., Optics Express 12 (25) (2004) 6299.
[18] L. Melnikov, I. Khromova, A. Sherbakov, N. Nikishin, Proceedings of SPIE 5950 (2005) 243.
[19] Y.-Ch. Hsue, T.-J. Yang, A novel view of plane wave expansion method in PCs, 2003. arxiv:/uk.arXiv.org>physics>arXiv:physics/0307150v1.
[20] R. Kotynski, Optical and Quantum Electronics 37 (2005) 253.
[21] F. Couny, F. Benabid, P.S. Light, Optics Letters 31 (24) (2006) 3574.
[22] J. Sun, C.C. Chan, Optics Letters 32 (14) (2007) 1989.
[23] I.A. Khromova, L.A. Melnikov, LC infiltrated photonic bandgap fibers: Dispersion and mode characteristics calculation, Technical Digest of Conference "LOYS-2006", ThS7–03, 2006, p. 99.
[24] I.A. Khromova, L.A. Melnikov, Dispersion properties of PCs and photonic band gap fibers with anisotropic elements, Proceedings of 13th Student Seminar on Microwave Applications of Novel Physical Phenomena, 2006, p. 38.

Please cite this article in press as: I.A. Khromova, L.A. Melnikov, Opt. Commun. (2008), doi:10.1016/j.optcom.2008.07.059